electronics

MDPI

Article

5G Cellular Networks: Coverage Analysis in the Presence of Inter-Cell Interference and Intentional Jammers

Muhammad Qasim [1], Muhammad Sajid Haroon [2], Muhammad Imran [1], Fazal Muhammad [3] and Sunghwan Kim [4,*]

1 Department of Electrical Engineering, Military College of Signals, National University of Sciences and Technology, Islamabad 44000, Pakistan; mqasim4@gmail.com (M.Q.); m.imran@mcs.edu.pk (M.I.)
2 Faculty of Electrical Engineering, GIK Institute of Engineering Sciences and Technology, Topi 23460, Pakistan; sajidiiui222@gmail.com
3 Department of Electrical Engineering, City University of Science and Information Technology, Peshawar 25000, Pakistan; fazal.muhammad@cusit.edu.pk
4 School of Electrical Engineering, University of Ulsan, Ulsan 44610, Korea
* Correspondence: sungkim@ulsan.ac.kr; Tel.: +82-52-259-1401

Received: 29 July 2020; Accepted: 18 September 2020; Published: 20 September 2020

Abstract: Intentional jammers (IJs) can be used by attackers for the launching of distributed denial-of-service attacks in 5G cellular networks. These adversaries are assumed to have adequate information about the network specifications, such as duration, transmit power and positions. With these assumptions, the IJs gain the ability to disrupt the legitimate communication of the network. Heterogeneous cellular networks (HetNets) can be considered a vital enabler for 5G cellular networks. Small base stations (SBSs) are deployed inside macro base station (MBS) to improve spectral efficiency and capacity. Due to orthogonal frequency division multiplexing assumption, HetNets' performance is mainly limited by inter-cell interference (ICI). Additionally, there exist IJs-interference (IJs-I), which significantly degrades the network coverage depending on the IJs' transmit power levels and their proximity with the target. The proposed work explores the uplink (UL) coverage performance of HetNets in the presence of both IJs-I and ICI. Moreover, to reduce the effects of ICI and IJs-I, reverse frequency allocation (RFA) is employed which is a proactive interference abating scheme. In RFA, different sub-bands of the available spectrum are used by MBS and SBS in alternate regions. The proposed setup is evaluated both analytically as well as with the help of simulation. The results demonstrate considerable UL coverage performance improvement by effectively mitigating IJs-I and ICI.

Keywords: coverage probability; denial-of-service; heterogeneous cellular networks; inter-cell interference; poisson point process; reverse frequency allocation; jammers

1. Introduction

1.1. Motivation

1.1.1. Increased Reliance on Wireless Communication

Today, wireless communication has transformed our lives. In past decade, our reliance on wireless communication has increased many times [1,2]. It has made our lives easier due to its usefulness and effectiveness. Social networks and video streaming applications have increased our reliance on smart phones that leads to increased traffic load on cellular networks. Exponentially growing demand

for high data rates and ubiquitous coverage requires the wireless network providers to boost both network's capacity and coverage.

In recent times, data usage has grown about 200% and, thus, leverages Internet of Things (IoT) in Heterogeneous cellular networks (HetNets) [1–3]. As a result, the network operators are now looking for more flexible and advanced network topologies, to satisfy user demands [2].

1.1.2. Using HetNets

Traditional homogeneous networks face great challenges in order to meet the ever-increasing demand of data. Therefore, HetNets must be used to cater for the data requirements. Different wireless access technologies with separate constraints and capabilities are part of HetNets.

For HetNets, coverage, bandwidth quality and performance is improved by implementation of ultra-dense Small base stations (SBSs) within the region served by Macro base station (MBS), as seen in Figure 1 [2,4]. Orthogonal frequency division multiple access (OFDMA) provides multiple access by assigning each user a subsets of sub-carriers, allowing simultaneous transmission from several users. The usage of OFDMA in HetNets significantly reduces Inter-cell interference (ICI) which is a significant limiting factor in improving coverage in HetNets because it significantly decrease the coverage of MBS edge-users (M-EUs) in HetNets [3].

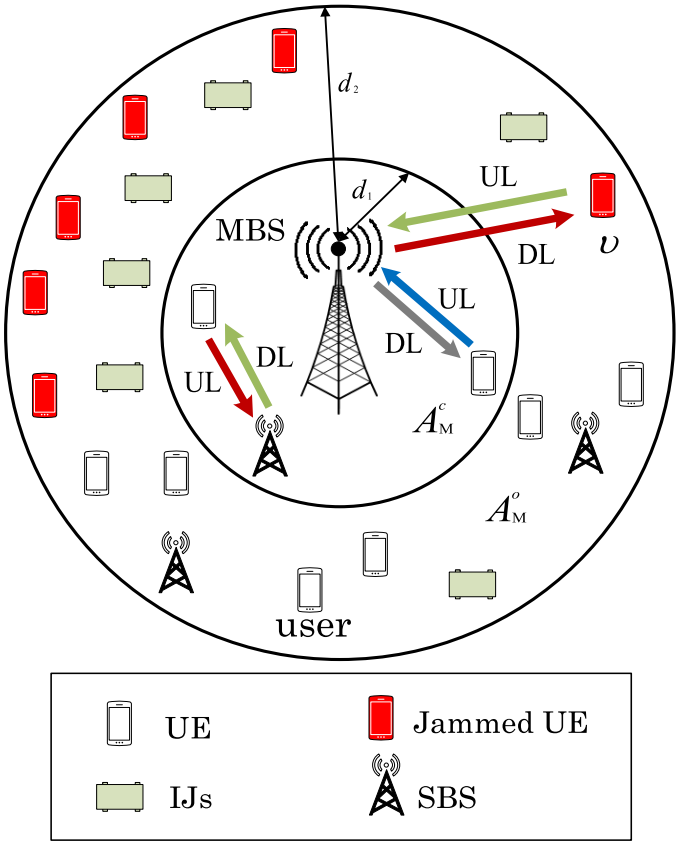

Figure 1. HetNet with RFA and IJs in two-tier. MBS, SBSs, users and IJs follow IHPPPs.

1.1.3. Distributed Denial-of-Service Attacks

As the importance of communication in our daily lives is increasing, we are more prone to being target of Distributed denial-of-service (DDoS) attacks which can blackout our communications. DDoS is a rapidly growing problem. The multitude and variety of both the attacks and the defense approaches is overwhelming [5]. Low transmit power levels of user in uplink (UL) communications renders it more prone to DDoS attacks [6,7]. Therefore, this work investigates Intentional jammers (IJs) attacks to reduce target's UL Signal Interference Ratio (SIR) [8].

1.1.4. Intentional Jammers and Inter-Cell Interference

Generally, IJs' attacks the public attractions places in MBS coverage area to reduce network coverage. The IJs try to degrade the UL communications by adding significant IJs-interference (IJs-I) in the communication system [9,10]. However, the transmit power of IJs are limited due to their wide-band nature and distance to the target [9]. Hence, for the IJs to be effective, they are required to be deployed near the target in sufficient number and in close proximity [11]. Moreover, this work consider that the IJs possesses necessary details about network parameters including location of target, transmit power and frequency band, thus, forcing the target out of coverage [9,12,13].

Independent homogeneous Poisson point processes (IHPPPs) are widely used to distribute MBSs, SBSs and users in HetNets due to tractability and ease of analysis [2–4]. In HetNets, OFDMA employment give rise to no/limited ICI; however, ICI remains the main performance limiting attribute [14,15]. In Non-uniform HetNets (NU-HetNets), users and MBSs are deployed via IHPPP while distribution of SBSs is through Poisson hole process. NU-HetNets lead to lower ICI and thus improves the performance of network coverage [16,17].

1.1.5. Interference Reduction Schemes

Research has been carried out on different interference reduction systems such as Fractional frequency reuse (FFR) [18] and Soft frequency reuse (SFR) [19]. The SFR system achieves higher spectral efficiency due to frequency reuse, and FFR contributes to reduced interference because of partitioning [20] of the overall usable bandwidth. Reverse frequency allocation (RFA) [14,19] is another proactive resource management system which helps in reducing interference. Through RFA the maximum bandwidth is made usable in a cell for both MBS and SBS. Consequently, spectral efficiency of RFA is more than SFR and FFR.

1.1.6. Proposed Work

In this work, RFA will be used in HetNets to abate ICI and IJs-I and, thus, improve UL coverage performance in HetNets. The proposed network setup promises higher network capacity by effectively reducing ICI and IJs-I in HetNets. To support this study, we have provided list of acronyms in Table 1 and notation summary in Table 2.

Table 1. List of acronyms.

Acronym	Description
IJs	Intentional jammers
HetNets	Heterogeneous cellular networks
SBSs	Small base stations
MBS	Macro base station
IJs-I	IJs-interference
UL	Uplink
RFA	Reverse frequency allocation
IoT	Internet of things
ICI	Inter-cell interference
NU-HetNets	Non-uniform HetNets
FFR	Fractional frequency reuse
SFR	Soft frequency reuse
DL	Downlink
NOMA	Non-orthogonal multiple access
5G	Fifth-generation
M-EUs	MBS edge-users
LT	Laplace transform
DDoS	Distributed denial-of-service
SIR	Signal-to-interference ratio

Table 2. Notation summary.

Notation	Description
ρ_{M}, ρ_{S}, ρ_u, ρ_J	IHPPPs of MBSs, SBSs, users, and IJs, respectively
Γ_{M}	SIR threshold
d_1, d_2	Radius of A^c_{M} and A^o_{M}, respectively
ρ_{M}, ρ_{S} and ρ_j	Densities of MBSs, SBSs, and IJs, respectively
β	Path loss exponent, $\forall\ \beta_{\mathrm{M}} = \beta_{\mathrm{S}} = \beta$, and $\beta > 2$
ν	Typical user
$*$	Denotes RFA employment
$\gamma_\circ$	Ratio of $P_{t,\mathrm{M}}$ and $P^{\mathrm{UL}}_{t,\nu}$
γ_1	Ratio of $P_{t,\mathrm{S}}$ and $P^{\mathrm{UL}}_{t,\nu}$
γ_2	Ratio of $P_{t,J}$ and $P^{\mathrm{UL}}_{t,\nu}$
γ_3	Ratio of $P^{\mathrm{DL}}_{t,\mathrm{S}}$ and $P^{\mathrm{UL}}_{t,\nu}$

1.2. Related Work

Different types of jamming attacks are studied by the authors in [21]. These include, wide-band jammers, noise jammers, partial band jammers, equalization jamming, and automatic gain control jamming. Additionally, the work investigates different jamming attack techniques and various types of targets. They conclude that advanced and sophisticated jamming techniques are required to jam the more complex wireless systems. In [22], deep recurrent and deep convolutional neural networks are used for detecting the jamming attacks. Their proposed model leads to 85% accuracy in jamming detection and classification. In [23], multiple-input and multiple-output (MIMO) networks have been probed by authors in the presence of advanced jamming attacks. Their proposed model assumes that the jammers can increase their transmit power levels to cause severe network performance degradation. Moreover, they investigate different jamming attack scenarios in MIMO networks and their effectiveness. In [24], challenges in jamming aware MIMO decision fusion channel along with distributed detection in wireless sensor networks over fading channels have been discussed. Jamming suppression capability of the proposed system has also been highlighted in the paper.

For the RFA employment in HetNets and its effective performance evaluation, two non-overlapping regions have been formed from coverage region of MBS, consisting of center, A^c_k, and outer region, A^o_k, $\forall k \in \{\mathrm{M}, \mathrm{S}\}$ [14,25]. The authors in [14], use RFA and load balancing to mitigate ICI. Their results indicate significant coverage performance improvement for MBS edge user by using their proposed setup. NU-HetNets along with SFR is investigated in [19]. The coverage probability expressions have been derived by the authors while assuming both U-HetNets and NU-HetNets. Their outcomes suggest that NU-HetNets along with SFR results in significant coverage improvement due to effective ICI mitigation. In [26], a novel technique for SBS deployment is proposed, where the SBSs are powered on via renewable energy source. The authors termed this approach as off-grid NU-HetNets, where the SBS are not grid connected. Moreover, HetNets' performance is evaluated by considering off-grid SBSs and on-grid MBSs. They derive expressions for coverage probability, association probabilities, and distance distribution while considering the proposed setup. Their results indicate that off-grid SBSs provide lower coverage due to limited available power. NU-HetNets with non-orthogonal multiple access (NOMA) is investigated in [17]. The work evaluates energy efficiency and downlink (DL) coverage for the proposed model. Results show that employment of NOMA leads to higher rate coverage and energy efficiency in HetNets. Similarly, NU-HetNet in conjunction with RFA is considered in [27]. In this work, SBSs are assumed to

be muted near MBS to avoid significant co-tier interference. However, SBSs are kept active in MBS edge area to improve edge user coverage. Moreover, the authors characterize both rate and coverage analyses for the proposed setup. The results show that NU-HetNets in MBS coverage edge area improve the network coverage and rate. In [28], variants of RFA are proposed to improve network coverage performance. Through results, the authors show that the variants of RFA lead to significant coverage improvement due to effective resource use.

The work in [29] discusses the growing trend of IoT integration with fifth-generation (5G) networks. Moreover, the authors also evaluate the security aspects of IoT-5G integration. Similarly, in [30], the authors discuss evolution of 5G-assisted IoT. Furthermore, they evaluate the future trends, key enabling technologies, and challenges for 5G assisted IoT.

In [31], the authors have proposed the architecture of IoT e-Health system to provide seamless connection of patients, hospitals and services. Moreover, various challenges to IoT including privacy, security and data management have also been elaborated. Moreover, in [32], proposal for ensuring public safety in smart cities by detecting radioactive nuclear source with inexpensive radiation counters have been discussed.

This proposal differs from the state-of-the-art in following ways:

1. Works in [21–23] explore different jamming attacks in different network types; however, they lack the evaluation of IJs in HetNets. Therefore, in this work, the IJs in HetNets are investigated.
2. The works in [14,17,19,25–28] investigate the mitigation of ICI by RFA in HetNets. However, they lack the use of RFA to abate IJs-I. Therefore, in this work, RFA is employed to mitigate both ICI and IJs-I.
3. In [17,27,28], DL coverage analysis is performed, while the focus of this work is on analyzing the bottleneck UL coverage analysis of the MBS edge user.

1.3. Contributions and Objectives

The research objectives that can be obtained from the proposed work are given below.

1. Investigation of the disruption caused by IJs' attacks to the legitimate UL communication in HetNets.
2. The mitigation of both ICI and IJs-I for the improvement of network performance gain. For this, among the best available techniques such as RFA is employed.
3. This work focuses on increasing capacity and coverage of the network and, thus, renders HetNets as a key enabler for future 5G.
4. To make the network more resilient to both ICI and IJs-I. This can be achieved by efficient resource use via RFA.
5. To investigate UL coverage for the proposed setup against different network parameters, such as SBS density, IJs' density, and SIR threshold.

The rest of paper is organized as follows. Section 2 explains the system model. Derivation of coverage probabilities has been discussed in Section 3. Section 4 contains discussion on results of the proposed system. Lastly Section 5, concludes the paper.

2. System Model

Network layout along with the interference mitigation schemes used has been introduced in this section. Moreover, network assumptions, IJs' attack mechanism and RFA are discussed here. Furthermore, mathematical preliminaries obtained here are also used in Section 3 for coverage probabilities derivation.

2.1. Network Layout and Assumptions

HetNet model with two tiers is considered, which includes MBSs, SBSs, user, and IJs. MBSs, SBSs, users, and IJs are distributes via IHPPPs with densities ρ_{M}, ρ_{S}, ρ_u and ρ_{J}, respectively. For the IJs are assumed to be transmitting unwanted energies in the legitimate communication band and, thus, degrade the network performance. To mitigate ICI and IJs-I, a proactive interference abating scheme, i.e., RFA is employed. A typical user has been considered for analysis. β denotes the path loss exponents while $|h|$ denotes Rayleigh fading gain. Moreover, the association of users carried out via maximum received power scheme [33].

2.2. IJs Mechanism

IJs transmit noise energy to reduce network coverage by targeting the legitimate communications [21]. In addition, we consider IJs to be low-cost and lightweight transmitters which are deployed randomly via IHPPP throughout the MBS coverage region. Severe degradation is experienced in M-EUs UL communication because of ICI and M-EUs enhanced distance from the MBS. Desired communication frequency can be jammed by IJs.

Because of its wide-band existence, the noise power can be as low as the UL transmit power of UE and does hardly any harm in the presence of a few IJs. Considerable IJs-I is achieved as the density and power of the IJs increases, and thus degrades the network's performance [8,22]. More precisely, by increasing density of IJs and transmission capacity, UL contact of M-EUs in HetNets can be completely blocked.

2.3. Reverse Frequency Allocation

High throughput is achieved in HetNet with the help of frequency reuse; however, according to SFR, frequency band is divided into two sub-bands. The users and SBSs in the MBS A^{c}_{M} will be allocated one sub-band while the second sub-band will be used by SBSs and users in the A^{o}_{M} [34].

RFA is the evolved version of SFR with improved coverage performance [35]. In contrast to SFR, the frequency sub-bands in RFA are further split into UL and DL frequencies and, thus, enables significant interference reduction than SFR [28,35]. The direction of radio transmissions of MBS are allotted to SBSs in reverse fashion, i.e., the UL frequencies of MBS are allotted as DL frequencies of SBS and DL frequencies of MBS are used as UL frequencies of SBSs [36]. Such frequency allocation mechanism enables the RFA to significantly improves network capacity over the entire MBS coverage region. Therefore, RFA is used to effectively mitigate the interference and, thus, increases spectral efficiency and network coverage. Frequency resources are allocated optimally which introduces lower co-tier and cross-tier interference which result in enhanced data rates [37].

RFA-based network partitioning eliminates interference and increases coverage, because no fixed spectrum allocation is assigned to SBS. Therefore, employment of RFA can make the entire spectrum of MBS available to SBSs in non-overlapping regions and reverse direction.

As shown in Figure 2, sub-bands used in SBSs and MBSs for RFA are in reverse order for A^{g}_{l} $\forall\, l \in (\mathrm{M},\mathrm{S})$ and $g \in (c,o)$.

In RFA, the allocated frequency, F, is subdivided into two bands, F_1 and F_2, such that $\mathrm{F} = \bigcup_{z\in(1,2)} \mathrm{F}z$, as shown in Figure 2. Sub-bands F1 and F2 are further divided into sub-carriers DL and UL, and are modeled as $\mathrm{F}_1 = \mathrm{F}_{1,\mathrm{DL}} + \mathrm{F}_{1,\mathrm{UL}}$ and $\mathrm{F}_2 = \mathrm{F}_{2,\mathrm{DL}} + \mathrm{F}_{2,\mathrm{UL}}$, respectively.

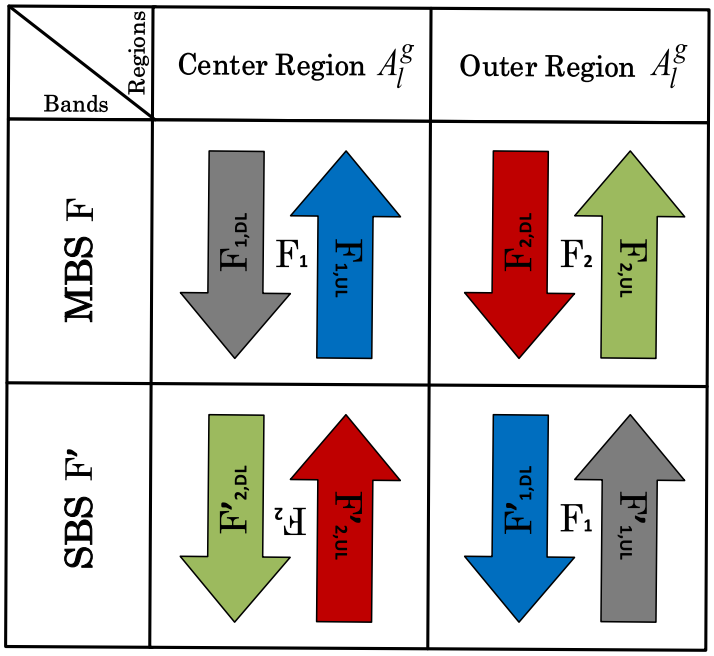

Figure 2. Two-tier HetNet model with RFA.

3. Coverage Probability Analysis

In this section, coverage probabilities expressions for undermentioned network scenarios are extracted, since ν is located in A_{M}^{c} and A_{M}^{o}; (i) coverage probability for UL in the presence of IJs without RFA (ii) coverage probability for UL in the presence of IJs with RFA.

3.1. Coverage Probability for UL in the Presence of IJs without RFA

In HetNet, it is presumed that to degrade the M-EUs' UL communication , IJs are deployed uniformly around the MBS coverage area using IHPPP. Therefore, in such a network environment IJs-I and ICI are the main efficiency limiting factors. The expression for UL coverage probability, $P_{A_{\mathrm{M}}^{c}}^{\mathrm{UL}}(\Gamma_{\mathrm{M}})$, for MBS associated ν in A_{M}^{c} with IJs without RFA may be expressed as

$$P_{A_{\mathrm{M}}^{c}}^{\mathrm{UL}}(\Gamma_{\mathrm{M}}) = P\left(\mathrm{SIR}_{\mathrm{M}}^{\mathrm{UL}} > \Gamma_{\mathrm{M}}\right). \tag{1}$$

Here, Γ_{M} is the UL SIR threshold, while $\mathrm{SIR}_{\mathrm{M}}^{\mathrm{UL}}$ indicates the received UL SIR. $\mathrm{SIR}_{\mathrm{M}}^{\mathrm{UL}}$ from (1) can be written as

$$\begin{aligned}\mathrm{SIR}_{\mathrm{M}}^{\mathrm{UL}} &= \frac{P_{t,\nu}^{\mathrm{UL}}|h_{\mathrm{M}}|^2 r_{\mathrm{M}}^{-\beta}}{I_{\mathrm{M},A} + I_{\mathrm{S},A} + I_{J,A}}, \\ &= \frac{P_{t,\nu}^{\mathrm{UL}}|h_{\mathrm{M}}|^2 r_{\mathrm{M}}^{-\beta}}{\sum\limits_{l\in\phi_{\mathrm{M}}} P_{t,l}|h_l|^2 r_l^{-\beta} + \sum\limits_{k\in\phi_{\mathrm{S}}} P_{t,k}|h_k|^2 r_k^{-\beta} + \sum\limits_{j\in\phi_J} P_{t,j}|h_j|^2 r_j^{-\beta}}.\end{aligned} \tag{2}$$

In (2), the UL interference in A_{M}^{c} is the accumulate interferences from (i) MBS-tier, $I_{\mathrm{M},A}$, (ii) SBS-tier, $I_{\mathrm{S},A}$, and (iii) IJs, $I_{J,A}$. $r_{(\cdot)}^{-\beta}$ indicates the distance from IJs or BS. Moreover, $P_{t,\nu}^{\mathrm{UL}}$ is the transmit power in UL. $P_{t,l}$, $P_{t,k}$ and $P_{t,j}$ are the transmit powers of MBSs, SBSs and IJs, respectively. ϕ_{M}, ϕ_{S} and ϕ_J

are the IHPPPs of MBSs, SBSs and IJs, respectively. Moreover, A denotes the MBS coverage area, i.e., $A = A^{c}_{\mathrm{M}} \bigcup A^{o}_{\mathrm{M}}$. Using (2), (1) can be written as

$$\begin{aligned} P^{\mathrm{UL}}_{A^{c}_{\mathrm{M}}}(\Gamma_{\mathrm{M}}) &\overset{(1)}{=} P\left(\frac{P^{\mathrm{UL}}_{t,\nu}|h_{\mathrm{M}}|^{2} r_{\mathrm{M}}^{-\beta}}{I_{\mathrm{M},A} + I_{\mathrm{S},A} + I_{J,A}} > \Gamma_{\mathrm{M}}\right) \\ &\overset{(2)}{=} \mathrm{E}_{r_{\mathrm{M}}, I_{\mathrm{M},A}, I_{\mathrm{S},A}, I_{J,A}}\left[\exp\left(-\frac{r_{\mathrm{M}}^{\beta}\Gamma_{\mathrm{M}}}{P^{\mathrm{UL}}_{t,\nu}}\left(I_{\mathrm{M},A} + I_{\mathrm{S},A} + I_{J,A}\right)\right)\right] \\ &\overset{(3)}{=} \mathrm{E}_{r_{\mathrm{M}}, I_{\mathrm{M},A}, I_{\mathrm{S},A}, I_{J,A}}\left[\exp\left(-s\left(I_{\mathrm{M},A} + I_{\mathrm{S},A} + I_{J,A}\right)\right)\right] \\ &\overset{(4)}{=} \mathrm{E}_{r_{\mathrm{M}}}\left[\mathrm{E}_{I_{\mathrm{M},A}}\exp\left(-s\left(I_{\mathrm{M},A}\right)\right) \times \mathrm{E}_{I_{\mathrm{S},A}}\exp\left(-s\left(I_{\mathrm{S},A}\right)\right) \times \mathrm{E}_{I_{J,A}}\exp\left(-s\left(I_{J,A}\right)\right)\right] \\ &\overset{(5)}{=} \mathrm{E}_{r_{\mathrm{M}}}\left[\mathcal{L}_{I_{\mathrm{M},A}}(s) \times \mathcal{L}_{I_{\mathrm{S},A}}(s) \times \mathcal{L}_{I_{J,A}}(s)\right]\Big|_{s=\frac{r_{\mathrm{M}}^{\beta}\Gamma_{\mathrm{M}}}{P^{\mathrm{UL}}_{t,\nu}}}. \end{aligned} \tag{3}$$

Here, $\mathcal{L}_{I_{\mathrm{M},A}}(s)$, $\mathcal{L}_{I_{\mathrm{S},A}}(s)$, and $\mathcal{L}_{I_{J,A}}(s)$ denote the Laplace transform (LT) of $I_{\mathrm{M},A}$, $I_{\mathrm{S},A}$, and $I_{J,A}$, respectively. Moreover, $\mathrm{E}[\bullet]$ denotes the expectation of LTs.

In (3), Step (1) follows from the coverage probability definition [14]. Step (2) is obtained by using void probability of IHPPP. Step (3) is achieved by substituting $\frac{r_{\mathrm{M}}^{\beta}\Gamma_{\mathrm{M}}}{P^{\mathrm{UL}}_{t,\nu}}$ by s into Step (2). Moreover, Step (4) is obtained by using the exponential property of sums into products, i.e., $\exp(a+b) = \exp(a) \times \exp(b)$. Finally, Step (5) is obtained from Step (4) by using the definition of LT (see (2.12) of [3]).

The LT of interference received from MBS-tier, $\mathcal{L}_{I_{\mathrm{M},A}}(s)$, in A, is obtained as

$$\begin{aligned} \mathcal{L}_{I_{\mathrm{M},A}}(s) = \exp\Bigg(&\frac{\rho_{\mathrm{M}}\pi\gamma_{\circ}\Gamma_{\mathrm{M}} d_{2}^{(2-\beta)} r_{\mathrm{M}}^{\beta}}{\beta/2-1} {}_2F_1\left(1, 1-\frac{2}{\beta}, 2-\frac{2}{\beta}, -\gamma_{\circ}\Gamma_{\mathrm{M}}\left(\frac{r_{\mathrm{M}}}{d_2}\right)^{\beta}\right) - \\ &\frac{\rho_{\mathrm{M}}\pi\gamma_{\circ}\Gamma_{\mathrm{M}} y^{(2-\beta)} r_{\mathrm{M}}^{\beta}}{\beta/2-1} {}_2F_1\left(1, 1-\frac{2}{\beta}, 2-\frac{2}{\beta}, -\gamma_{\circ}\Gamma_{\mathrm{M}}\left(\frac{r_{\mathrm{M}}}{y}\right)^{\beta}\right)\Bigg). \end{aligned} \tag{4}$$

Proof. See Appendix A for the proof of (4). In (4), $\gamma_{\circ}$ is the ratio of $P_{t,\mathrm{M}}$ and $P^{\mathrm{UL}}_{t,\nu}$, where $P_{t,\mathrm{M}}$ is transmission power of MBS-tier. □

Using the same approach as of (4), A, can be determined by taking LT of the received interference from SBS-tier, $\mathcal{L}_{I_{\mathrm{S},A}}(s)$

$$\begin{aligned} \mathcal{L}_{I_{\mathrm{S},A}}(s) = \exp\Bigg(&\frac{\rho_{\mathrm{S}}\pi\gamma_{1}\Gamma_{\mathrm{M}} x_{2}^{(2-\beta)} r_{\mathrm{M}}^{\beta}}{\beta/2-1} {}_2F_1\left(1, 1-\frac{2}{\beta}, 2-\frac{2}{\beta}, -\gamma_{1}\Gamma_{\mathrm{M}}\left(\frac{r_{\mathrm{M}}}{x_2}\right)^{\beta}\right) - \\ &\frac{\rho_{\mathrm{S}}\pi\gamma_{1}\Gamma_{\mathrm{M}} x_{1}^{(2-\beta)} r_{\mathrm{M}}^{\beta}}{\beta/2-1} {}_2F_1\left(1, 1-\frac{2}{\beta}, 2-\frac{2}{\beta}, -\gamma_{1}\Gamma_{\mathrm{M}}\left(\frac{r_{\mathrm{M}}}{x_1}\right)^{\beta}\right)\Bigg). \end{aligned} \tag{5}$$

Here, γ_1 is ratio of $P_{t,\mathrm{S}}$ and $P^{\mathrm{UL}}_{t,\nu}$, where $P_{t,\mathrm{S}}$ is the transmit power of SBS.

Similarly, using the same approach as of (4), the LT of the interference received from IJs, $\mathcal{L}_{I_{J,A}}(s)$, in A, can be given as

$$\mathcal{L}_{I_{J,A}}(s) = \exp\left(\frac{\rho_J \pi \gamma_2 \Gamma_{\mathrm{M}} z_2^{(2-\beta)} r_{\mathrm{M}}^{\beta}}{\beta/2-1} {}_2F_1\left(1, 1-\frac{2}{\beta}, 2-\frac{2}{\beta}, -\gamma_2\Gamma_{\mathrm{M}}\left(\frac{r_{\mathrm{M}}}{z_2}\right)^{\beta}\right) - \frac{\rho_J \pi \gamma_2 \Gamma_{\mathrm{M}} z_1^{(2-\beta)} r_{\mathrm{M}}^{\beta}}{\beta/2-1} {}_2F_1\left(1, 1-\frac{2}{\beta}, 2-\frac{2}{\beta}, -\gamma_2\Gamma_{\mathrm{M}}\left(\frac{r_{\mathrm{M}}}{z_1}\right)^{\beta}\right)\right). \tag{6}$$

Here, γ_2 is the ratio of $P_{t,J}$ and $P_{t,\nu}^{\mathrm{UL}}$ where $P_{t,J}$ is the transmit power of IJs and z_1 and z_2 define the effective attacking areas of the jammers, s.t., $z_1 \leq z_2$.

ν is located in A_{M}^{c} or in A_{M}^{o} (denoted as $\nu_{A_{\mathrm{M}}^{c}}$ and $\nu_{A_{\mathrm{M}}^{o}}$, respectively), while associated with MBS at a distance $r_{\mathrm{M},\nu}$, has PDFs of distances given, respectively, as (7) and (8) [35,38]

$$f_{r_{\mathrm{M}}|\nu_{A_{\mathrm{M}}^{c}}}(r_{\mathrm{M}}) = \frac{2\pi\rho_{\mathrm{M}} r_{\mathrm{M}} \exp\left(-\rho_{\mathrm{M}}\pi r_{\mathrm{M}}^2\right)}{1-\exp\left(-\rho_{\mathrm{M}}\pi d_1^2\right)}, \tag{7}$$

and

$$f_{r_{\mathrm{M}}|\nu_{A_{\mathrm{M}}^{o}}}(r_{\mathrm{M}}) = \frac{2\pi\rho_{\mathrm{M}} r_{\mathrm{M}} \exp\left(-\rho_{\mathrm{M}}\pi r_{\mathrm{M}}^2\right)}{\exp\left(-\rho_{\mathrm{M}}\pi d_1^2\right)}. \tag{8}$$

UL coverage probability expression, $P_{A_{\mathrm{M}}^{c}}^{\mathrm{UL}}(\Gamma_{\mathrm{M}})$, for MBS associated ν in A_{M}^{c} while considering uniform IJs distribution and without RFA employment, can be achieved as

$$P_{A_{\mathrm{M}}^{c}}^{\mathrm{UL}}(\Gamma_{\mathrm{M}}) = \int_{y}^{d_1} \mathcal{L}_{I_{\mathrm{M},A}}(s) \times \mathcal{L}_{I_{\mathrm{S},A}}(s) \times \mathcal{L}_{I_{J,A}}(s) f_{r_{\mathrm{M},\nu}|\nu_{A_{\mathrm{M}}^{c}}}(r_{\mathrm{M},\nu})\, dr_{\mathrm{M},\nu}. \tag{9}$$

By substituting (4)–(7) into (9), $P_{A_{\mathrm{M}}^{c}}^{\mathrm{UL}}(\Gamma_{\mathrm{M}})$ is achieved as (11).

Similarly, for uniformly distributed IJs without RFA, UL coverage probability expression, $P_{A_{\mathrm{M}}^{o}}^{\mathrm{UL}}(\Gamma_{\mathrm{M}})$, for MBS associated ν in A_{M}^{o} can be written as

$$P_{A_{\mathrm{M}}^{o}}^{\mathrm{UL}}(\Gamma_{\mathrm{M}}) = \int_{d_1}^{d_2} \mathcal{L}_{I_{\mathrm{M},A}}(s) \times \mathcal{L}_{I_{\mathrm{S},A}}(s) \times \mathcal{L}_{I_{J,A}}(s) f_{r_{\mathrm{M},\nu}|\nu_{A_{\mathrm{M}}^{o}}}(r_{\mathrm{M},\nu})\, dr_{\mathrm{M},\nu}. \tag{10}$$

By putting (4)–(6) and (8) in (10), $P_{A_{\mathrm{M}}^{o}}^{\mathrm{UL}}(\Gamma_{\mathrm{M}})$ is written as (12).

$$P_{A_{\mathrm{M}}^{c}}^{\mathrm{UL}}(\Gamma_{\mathrm{M}}) = \frac{2\pi\rho_{\mathrm{M}}}{1-\exp\left(-\rho_{\mathrm{M}}\pi d_1^2\right)} \int_{y}^{d_1} \exp\left(\frac{\pi\Gamma_{\mathrm{M}} r_{\mathrm{M}}^{\beta}}{\beta/2-1}\left[\rho_{\mathrm{M}}\gamma_{\circ} d_2^{(2-\beta)} \mathcal{J}\left(\beta, -\Gamma_{\mathrm{M}}\gamma_{\circ}\left(\frac{r_{\mathrm{M}}}{d_2}\right)^{\beta}\right) - \rho_{\mathrm{M}}\gamma_{\circ} y^{(2-\beta)} \mathcal{J}\left(\beta, -\Gamma_{\mathrm{M}}\gamma_{\circ}\left(\frac{r_{\mathrm{M}}}{y}\right)^{\beta}\right) + \rho_{\mathrm{S}}\gamma_1 x_2^{(2-\beta)} \mathcal{J}\left(\beta, -\Gamma_{\mathrm{M}}\gamma_1\left(\frac{r_{\mathrm{M}}}{x_2}\right)^{\beta}\right) - \rho_{\mathrm{S}}\gamma_1 x_1^{(2-\beta)} \mathcal{J}\left(\beta, -\Gamma_{\mathrm{M}}\gamma_1\left(\frac{r_{\mathrm{M}}}{x_1}\right)^{\beta}\right) + \rho_J\gamma_2 z_2^{(2-\beta)} \mathcal{J}\left(\beta, -\Gamma_{\mathrm{M}}\gamma_2\left(\frac{r_{\mathrm{M}}}{z_2}\right)^{\beta}\right) - \rho_J\gamma_2 z_1^{(2-\beta)} \mathcal{J}\left(\beta, -\Gamma_{\mathrm{M}}\gamma_2\left(\frac{r_{\mathrm{M}}}{z_1}\right)^{\beta}\right)\right] - \rho_{\mathrm{M}}\pi r_{\mathrm{M}}^2\right) r_{\mathrm{M}} dr_{\mathrm{M}}. \tag{11}$$

$$P^{\mathrm{UL}}_{A^o_{\mathrm{M}}}(\Gamma_{\mathrm{M}}) = \frac{2\pi\rho_{\mathrm{M}}}{\exp(-\rho_{\mathrm{M}}\pi d_1^2)} \int_{d_1}^{d_2} \exp\left(\frac{\pi\Gamma_{\mathrm{M}} r_{\mathrm{M}}^{\beta}}{\beta/2-1}\left[\rho_{\mathrm{M}}\gamma_{\circ} d_2^{(2-\beta)} \mathcal{J}\left(\beta, -\Gamma_{\mathrm{M}}\gamma_{\circ}\left(\frac{r_{\mathrm{M}}}{d_2}\right)^{\beta}\right) - \rho_{\mathrm{M}}\gamma_{\circ} y^{(2-\beta)} \mathcal{J}\left(\beta, -\Gamma_{\mathrm{M}}\gamma_{\circ}\left(\frac{r_{\mathrm{M}}}{y}\right)^{\beta}\right)\right.\right.$$

$$+\rho_{\mathrm{S}}\gamma_1 x_2^{(2-\beta)} \mathcal{J}\left(\beta, -\Gamma_{\mathrm{M}}\gamma_1\left(\frac{r_{\mathrm{M}}}{x_2}\right)^{\beta}\right) - \rho_{\mathrm{S}}\gamma_1 x_1^{(2-\beta)} \mathcal{J}\left(\beta, -\Gamma_{\mathrm{M}}\gamma_1\left(\frac{r_{\mathrm{M}}}{x_1}\right)^{\beta}\right) + \rho_J\gamma_2 z_2^{(2-\beta)} \mathcal{J}\left(\beta, -\Gamma_{\mathrm{M}}\gamma_2\left(\frac{r_{\mathrm{M}}}{z_2}\right)^{\beta}\right) - \quad (12)$$

$$\left.\left.\rho_J\gamma_2 z_1^{(2-\beta)} \mathcal{J}\left(\beta, -\Gamma_{\mathrm{M}}\gamma_2\left(\frac{r_{\mathrm{M}}}{z_1}\right)^{\beta}\right)\right] - \rho_{\mathrm{M}}\pi r_{\mathrm{M}}^2\right) r_{\mathrm{M}} dr_{\mathrm{M}}.$$

3.2. Coverage Probability for UL in the Presence of IJs with RFA

The expression for UL coverage probability, $P^{\mathrm{UL},*}_{A^c_{\mathrm{M}}}(\Gamma_{\mathrm{M}})$, with IJs and RFA while considering ν in A^c_{M} can be expressed as

$$P^{\mathrm{UL},*}_{A^c_{\mathrm{M}}}(\Gamma_{\mathrm{M}}) = P\left(\mathrm{SIR}^{\mathrm{UL}}_{\mathrm{M}} > \Gamma_{\mathrm{M}}\right). \quad (13)$$

The UL interference experienced while employing RFA, is the aggregate of MBS-tier UL interference in A^c_{M}, i.e., $I^{\mathrm{UL}}_{\phi_{\mathrm{M}},A^c_{\mathrm{M}}}$, SBS-tier DL interference in A^o_{M}, i.e., $I^{\mathrm{DL}}_{\phi_i,A^o_{\mathrm{M}}}$, and interference from IJs, i.e., $I_{J,A}$. Therefore, $\mathrm{SIR}^{\mathrm{UL}}_{\mathrm{M}}$ from (13) can be written as

$$\mathrm{SIR}^{\mathrm{UL}}_{\mathrm{M}} = \frac{P^{\mathrm{UL}}_{t,\nu}|h_{\mathrm{M}}|^2 r_{\mathrm{M}}^{-\beta}}{I^{\mathrm{UL}}_{\phi_{\mathrm{M}},A^c_{\mathrm{M}}} + I^{\mathrm{DL}}_{\phi_{\mathrm{S}},A^o_{\mathrm{M}}} + I_{J,A}}. \quad (14)$$

Equation (14) can be expanded as

$$\mathrm{SIR}^{\mathrm{UL}}_{\mathrm{M}} = \frac{P^{\mathrm{UL}}_{t,\nu}|h_{\mathrm{M}}|^2 r_{\mathrm{M}}^{-\beta}}{\sum\limits_{l\in\phi_{\mathrm{M}}} P^{\mathrm{UL}}_{t,l}|h_l|^2 r_l^{-\beta} + \sum\limits_{k\in\phi_{\mathrm{S}}} P^{\mathrm{DL}}_{t,k}|h_k|^2 r_k^{-\beta} + \sum\limits_{j\in\phi_J} P_{t,j}|h_j|^2 r_j^{-\beta}}. \quad (15)$$

Here, MBS UL transmit power of ν is, $P^{\mathrm{UL}}_{t,l}$, SBS DL transmit power is $P^{\mathrm{DL}}_{t,k}$, and IJs transmit power is $P_{t,j}$. Furthermore, by putting (14) in (13), we get $P^{\mathrm{UL},*}_{A^c_{\mathrm{M}}}(\Gamma_{\mathrm{M}})$ as

$$\begin{aligned} P^{\mathrm{UL},*}_{A^c_{\mathrm{M}}}(\Gamma_{\mathrm{M}}) &= P\left(\frac{P^{\mathrm{UL}}_{t,\nu}|h_{\mathrm{M}}|^2 r_{\mathrm{M}}^{-\beta}}{I^{\mathrm{UL}}_{\phi_{\mathrm{M}},A^c_{\mathrm{M}}} + I^{\mathrm{DL}}_{\phi_{\mathrm{S}},A^o_{\mathrm{M}}} + I_{J,A}} > \Gamma_{\mathrm{M}}\right) \\ &= \mathrm{E}_{r_{\mathrm{M}},I^{\mathrm{UL}}_{\phi_{\mathrm{M}},A^c_{\mathrm{M}}},I^{\mathrm{DL}}_{\phi_{\mathrm{S}},A^o_{\mathrm{M}}},I_{J,A}}\left[\exp\left(-\frac{r_{\mathrm{M}}^{\beta}\Gamma_{\mathrm{M}}}{P^{\mathrm{UL}}_{t,\nu}}\left(I^{\mathrm{UL}}_{\phi_{\mathrm{M}},A^c_{\mathrm{M}}} + I^{\mathrm{DL}}_{\phi_{\mathrm{S}},A^o_{\mathrm{M}}} + I_{J,A}\right)\right)\right] \\ &= \mathrm{E}_{r_{\mathrm{M}}}\left[\mathcal{L}_{I^{\mathrm{UL}}_{\phi_{\mathrm{M}},A^c_{\mathrm{M}}}}(s) \times \mathcal{L}_{I^{\mathrm{DL}}_{\phi_{\mathrm{S}},A^o_{\mathrm{M}}}}(s) \times \mathcal{L}_{I_{J,A}}(s)\right]\Big|_{s=\frac{r_{\mathrm{M}}^{\beta}\Gamma_{\mathrm{M}}}{P^{\mathrm{UL}}_{t,\nu}}}. \end{aligned} \quad (16)$$

The LT of MBS UL interference in A^c_{M}, i.e., $\mathcal{L}_{I^{\mathrm{UL}}_{\phi_{\mathrm{M}},A^c_{\mathrm{M}}}}$, can be written as

$$\mathcal{L}_{I^{\mathrm{UL}}_{\phi_{\mathrm{M}},A^c_{\mathrm{M}}}} = \exp\left(\frac{\rho_{\mathrm{M}}\pi\Gamma_{\mathrm{M}} d_1^{(2-\beta)} r_{\mathrm{M}}^{\beta}}{\beta/2-1} {}_2F_1\left(1, 1-\frac{2}{\beta}, 2-\frac{2}{\beta}, -\Gamma_{\mathrm{M}}\left(\frac{r_{\mathrm{M}}}{d_1}\right)^{\beta}\right) - \right.$$
$$\left.\frac{\rho_{\mathrm{M}}\pi\Gamma_{\mathrm{M}} y^{(2-\beta)} r_{\mathrm{M}}^{\beta}}{\beta/2-1} {}_2F_1\left(1, 1-\frac{2}{\beta}, 2-\frac{2}{\beta}, -\Gamma_{\mathrm{M}}\left(\frac{r_{\mathrm{M}}}{y}\right)^{\beta}\right)\right). \quad (17)$$

Proof. See Appendix B for the proof of (17). □

Moreover, LT of SBS DL interference in A_{M}^{o}, i.e., $\mathcal{L}_{I_{\phi_{\mathrm{S}},A_{\mathrm{M}}^{o}}^{\mathrm{DL}}}$, can be written in a way similar to (17), and is given as

$$\mathcal{L}_{I_{\phi_{\mathrm{S}},A_{\mathrm{M}}^{o}}^{\mathrm{DL}}} = \mathcal{L}_{I_{\phi_{\mathrm{S}},A_{\mathrm{M}}^{c}}^{\mathrm{DL}}} = \exp\left(\frac{\rho_{\mathrm{S}}^{'}\pi\gamma_3\Gamma_{\mathrm{M}}x_2^{(2-\beta)}r_{\mathrm{M}}^{\beta}}{\beta/2-1}{}_2F_1\left(1,1-\frac{2}{\beta},2-\frac{2}{\beta},-\gamma_3\Gamma_{\mathrm{M}}\left(\frac{r_{\mathrm{M}}}{x_2}\right)^{\beta}\right)-\right.$$
$$\left.\frac{\rho_{\mathrm{S}}^{'}\pi\gamma_3\Gamma_{\mathrm{M}}x_1^{(2-\beta)}r_{\mathrm{M}}^{\beta}}{\beta/2-1}{}_2F_1\left(1,1-\frac{2}{\beta},2-\frac{2}{\beta},-\gamma_3\Gamma_{\mathrm{M}}\left(\frac{r_{\mathrm{M}}}{x_1}\right)^{\beta}\right)\right). \tag{18}$$

Here, $\mathcal{L}_{I_{\phi_{\mathrm{S}},A_{\mathrm{M}}^{o}}^{\mathrm{DL}}} = \mathcal{L}_{I_{\phi_{\mathrm{S}},A_{\mathrm{M}}^{c}}^{\mathrm{DL}}}$ because ρ_{S} in A_{M}^{c} is approximately equal to ρ_{S} in A_{M}^{o}. γ_3 is the ratio of $P_{t,S}^{\mathrm{DL}}$ and $P_{t,\nu}^{\mathrm{UL}}$ where $P_{t,S}^{\mathrm{DL}}$ is the SBSs DL transmit power.

From (17), LT of MBS DL interference in A_{M}^{o}, i.e., $\mathcal{L}_{I_{\phi_{\mathrm{M}},A_{\mathrm{M}}^{o}}^{\mathrm{UL}}}$, is obtained as

$$\mathcal{L}_{I_{\phi_{\mathrm{M}},A_{\mathrm{M}}^{o}}^{\mathrm{UL}}}(s) = \exp\left(\frac{\rho_{\mathrm{M}}\pi\Gamma_{\mathrm{M}}d_2^{(2-\beta)}r_{\mathrm{M}}^{\beta}}{\beta/2-1}{}_2F_1\left(1,1-\frac{2}{\beta},2-\frac{2}{\beta},-\Gamma_{\mathrm{M}}\left(\frac{r_{\mathrm{M}}}{d_2}\right)^{\beta}\right)-\right.$$
$$\left.\frac{\rho_{\mathrm{M}}\pi\Gamma_{\mathrm{M}}d_1^{(2-\beta)}r_{\mathrm{M}}^{\beta}}{\beta/2-1}{}_2F_1\left(1,1-\frac{2}{\beta},2-\frac{2}{\beta},-\Gamma_{\mathrm{M}}\left(\frac{r_{\mathrm{M}}}{d_1}\right)^{\beta}\right)\right). \tag{19}$$

$$P_{A_{\mathrm{M}}^{o}}^{\mathrm{UL},*}(\Gamma_{\mathrm{M}}) = \frac{2\pi\rho_{\mathrm{M}}}{1-\exp\left(-\rho_{\mathrm{M}}\pi d_1^2\right)}\int_{y}^{d_1}\exp\left(\frac{\pi\Gamma_{\mathrm{M}}r_{\mathrm{M}}^{\beta}}{\beta/2-1}\left[\rho_{\mathrm{M}}d_1^{(2-\beta)}\mathcal{J}\left(\beta,-\Gamma_{\mathrm{M}}\left(\frac{r_{\mathrm{M}}}{d_1}\right)^{\beta}\right)-\rho_{\mathrm{M}}y^{(2-\beta)}\mathcal{J}\left(\beta,-\Gamma_{\mathrm{M}}\left(\frac{r_{\mathrm{M}}}{y}\right)^{\beta}\right)+\right.\right.$$
$$\rho_{\mathrm{S}}^{'}\gamma_3 d_2^{(2-\beta)}\mathcal{J}\left(\beta,-\Gamma_{\mathrm{M}}\gamma_3\left(\frac{r_{\mathrm{M}}}{d_2}\right)^{\beta}\right)-\rho_{\mathrm{S}}^{'}\gamma_3 {d_1}^{(2-\beta)}\mathcal{J}\left(\beta,-\Gamma_{\mathrm{M}}\gamma_3\left(\frac{r_{\mathrm{M}}}{d_1}\right)^{\beta}\right)+\rho_J\gamma_2 d_2^{(2-\beta)}\mathcal{J}\left(\beta,-\Gamma_{\mathrm{M}}\gamma_2\left(\frac{r_{\mathrm{M}}}{d_2}\right)^{\beta}\right)- \tag{20}$$
$$\left.\left.\rho_J\gamma_2 y^{(2-\beta)}\mathcal{J}\left(\beta,-\Gamma_{\mathrm{M}}\gamma_2\left(\frac{r_{\mathrm{M}}}{y}\right)^{\beta}\right)\right]-\rho_{\mathrm{M}}\pi r_{\mathrm{M}}^2\right)r_{\mathrm{M}}dr_{\mathrm{M}}.$$

$$P_{A_{\mathrm{M}}^{o}}^{\mathrm{UL},*}(\Gamma_{\mathrm{M}}) = \frac{2\pi\rho_{\mathrm{M}}}{\exp\left(-\rho_{\mathrm{M}}\pi d_1^2\right)}\int_{d_1}^{d_2}\exp\left(\frac{\pi\Gamma_{\mathrm{M}}r_{\mathrm{M}}^{\beta}}{\beta/2-1}\left[\rho_{\mathrm{M}}d_2^{(2-\beta)}\mathcal{J}\left(\beta,-\Gamma_{\mathrm{M}}\left(\frac{r_{\mathrm{M}}}{d_2}\right)^{\beta}\right)-\rho_{\mathrm{M}}{d_1}^{(2-\beta)}\mathcal{J}\left(\beta,-\Gamma_{\mathrm{M}}\left(\frac{r_{\mathrm{M}}}{d_1}\right)^{\beta}\right)+\right.\right.$$
$$\rho_{\mathrm{S}}^{'}\gamma_3 d_1^{(2-\beta)}\mathcal{J}\left(\beta,-\Gamma_{\mathrm{M}}\gamma_3\left(\frac{r_{\mathrm{M}}}{d_1}\right)^{\beta}\right)-\rho_{\mathrm{S}}^{'}\gamma_3 y^{(2-\beta)}\mathcal{J}\left(\beta,-\Gamma_{\mathrm{M}}\gamma_3\left(\frac{r_{\mathrm{M}}}{y}\right)^{\beta}\right)+\rho_J\gamma_2 d_2^{(2-\beta)}\mathcal{J}\left(\beta,-\Gamma_{\mathrm{M}}\gamma_2\left(\frac{r_{\mathrm{M}}}{d_2}\right)^{\beta}\right)- \tag{21}$$
$$\left.\left.\rho_J\gamma_2 y^{(2-\beta)}\mathcal{J}\left(\beta,-\Gamma_{\mathrm{M}}\gamma_2\left(\frac{r_{\mathrm{M}}}{y}\right)^{\beta}\right)\right]-\rho_{\mathrm{M}}\pi r_{\mathrm{M}}^2\right)r_{\mathrm{M}}dr_{\mathrm{M}}.$$

UL coverage probability expression, $P_{A_{\mathrm{M}}^{c}}^{\mathrm{UL},*}(\Gamma_{\mathrm{M}})$, for MBS associated ν in A_{M}^{c} while considering uniformly deployed IJs and RFA employment can be written as

$$P_{A_{\mathrm{M}}^{c}}^{\mathrm{UL},*}(\Gamma_{\mathrm{M}}) = \int_{y}^{d_1}\mathcal{L}_{I_{\phi_{\mathrm{M}},A_{\mathrm{M}}^{c}}^{\mathrm{UL}}}(s)\times\mathcal{L}_{I_{\phi_{\mathrm{S}},A_{\mathrm{M}}^{o}}^{\mathrm{DL}}}(s)\times\mathcal{L}_{I_{J,A}}(s)\,f_{r_{\mathrm{M},\nu}|\nu_{A_{\mathrm{M}}^{c}}}(r_{\mathrm{M},\nu})\,dr_{\mathrm{M},\nu}. \tag{22}$$

By putting (6), (7), (17) and (18), in (22), $P_{A_{\mathrm{M}}^{c}}^{\mathrm{UL},*}(\Gamma_{\mathrm{M}})$ is expressed as (20).

Similarly, UL coverage probability expression, $P^{\mathrm{UL},*}_{A^o_{\mathrm{M}}}(\Gamma_{\mathrm{M}})$, for ν associated with MBS in A^o_{M}, with uniformly deployed IJs and RFA employment, can be given as

$$P^{\mathrm{UL},*}_{A^o_{\mathrm{M}}}(\Gamma_{\mathrm{M}}) = \int_{d_1}^{d_2} \mathcal{L}_{I^{\mathrm{UL}}_{\phi_{\mathrm{M}},A^o_{\mathrm{M}}}}(s) \times \mathcal{L}_{I^{\mathrm{DL}}_{\phi_{\mathrm{S}},A^c_{\mathrm{M}}}}(s) \times \mathcal{L}_{I_{J,A}}(s)\, f_{r_{\mathrm{M},\nu}|\nu_{A^o_{\mathrm{M}}}}(r_{\mathrm{M},\nu})\, dr_{\mathrm{M},\nu}. \tag{23}$$

By putting (6), (8), (18) and (19) in (23), $P^{\mathrm{UL},*}_{A^o_{\mathrm{M}}}(\Gamma_{\mathrm{M}})$ is expressed as (21).

4. Results and Discussion

Within this section, we explain UL coverage probability results for ν while considering (i) probability of UL coverage with IJs and without RFA employment, and (ii) probability of UL coverage with IJs and RFA employment. We obtained the results using MATLAB 2017a. MBSs, SBSs, users and IJs are treated as $A = \pi(500\ \mathrm{m})^2$,s.t., $A = A^c_{\mathrm{M}} \mathrm{U} A^o_{\mathrm{M}}$. In addition, the transmitting powers of MBS, SBS, ν, and IJs are assumed to be 60 dBm, 40 dBm, 20 dBm, and 20 dBm, respectively. Different parameters, such as $P^{\mathrm{UL}}_{t,\nu}$, ρ_J, ρ_{M}, ρ_{S}, Γ_{M}, and $P_{t,J}$, are analyzed against UL coverage given that ν is located in A^o_{M}. The simulation parameters for the proposed setup are listed in Table 3.

Table 3. Simulation Parameters.

Parameter	Configuration
Channel bandwidth	10 MHz
MBS, SBSs, IJs	IHPPPs
Code iterations	1000
A	$\pi \times (500\ \mathrm{m})^2$
ρ_{S}	$20/\pi(500\ \mathrm{m})^2$
ρ_{M}	$4/\pi(500\ \mathrm{m})^2$
ρ_J	$20/\pi(500\ \mathrm{m})^2$
Transmit powers of MBS, SBS, ν , and IJs	45 dBm, 33 dBm, 20 dBm, and 20 dBm, respectively

Figure 3 compares the probabilities of UL coverage in A^o_{M} versus different values of Γ_{M}. The figure refers to the fact that higher ρ_J values lead to significant IJs-I and therefore lower coverage. In addition, the figure shows that employment with RFA causes improved coverage in both the presence and absence of IJs. This is because effective interfering SBSs are reduced because of RFA.

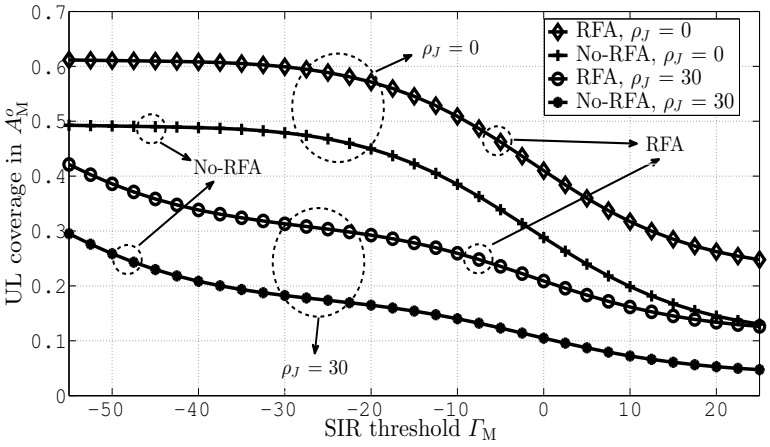

Figure 3. UL coverage versus Γ_{M} in A^o_{M}.

Figure 4 measures the probabilities of UL coverage in A^o_{M} versus different values of the Γ_{M} and ρ_J threshold. Generated for $\rho_J = 0, 20, 40, 60, 80, 100$. In the figure it can be observed that the coverage improves with RFA. This is due to RFA's efficient use of the resources and effective mitigation of interference. Increasing ρ_J also causes severe degradation of UL coverage due to significant IJs-I.

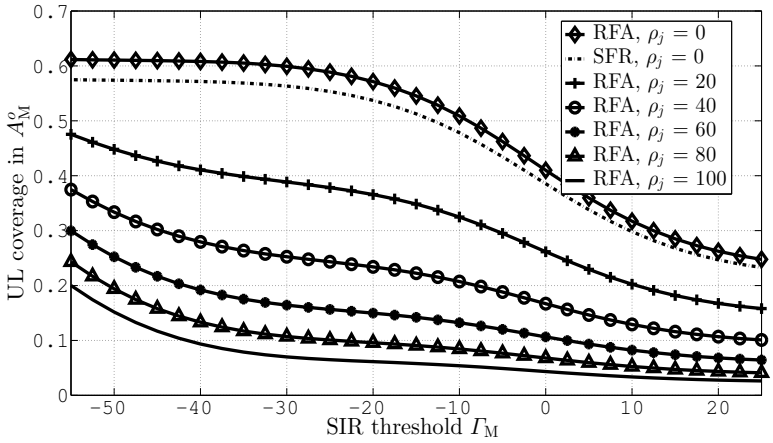

Figure 4. UL coverage against Γ_{M} and ρ_J in A^o_{M}.

At Figures 5 and 6, while assuming $\Gamma_{\mathrm{M}} = -40$ dB and $\rho_J = 20, 40, 60, 80$ and 100, we present UL coverage probabilities in A_{M} versus different IJs distribution area radius values. The results indicate that an increase in the distribution area of the IJs results in improved UL coverage due to a lower number of IJs per unit area, making the IJs less efficient as long as their transmission power is constant. Furthermore, due to efficient resource allocation RFA employment improves UL coverage.

Similarly, Figures 7 and 8 calculate UL coverage probabilities in A^o_{M} versus different IJs distribution area radius values while assuming $\rho_J = 60$ and $\Gamma_{\mathrm{M}} = -60, -40, 0$ and 20 dB. The results indicate that due to lower IJs-I, an increase in the distribution area of the IJs results in improved UL coverage. Furthermore, the results also show that higher values of Γ_{M} reduce UL coverage due to lower user associations.

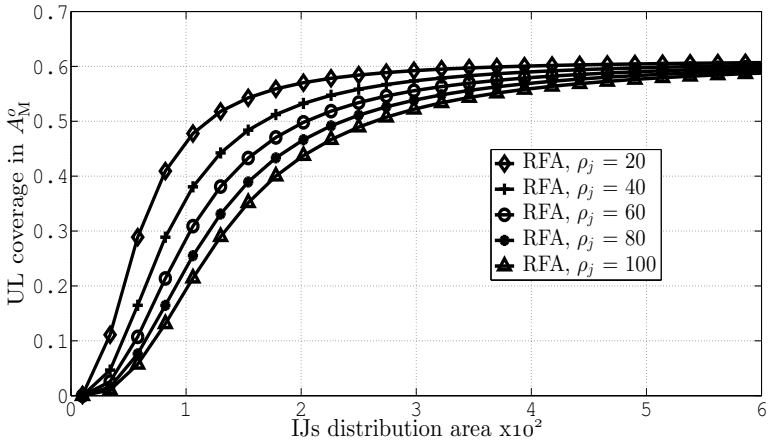

Figure 5. UL coverage against radius for IJs distribution area, with RFA.

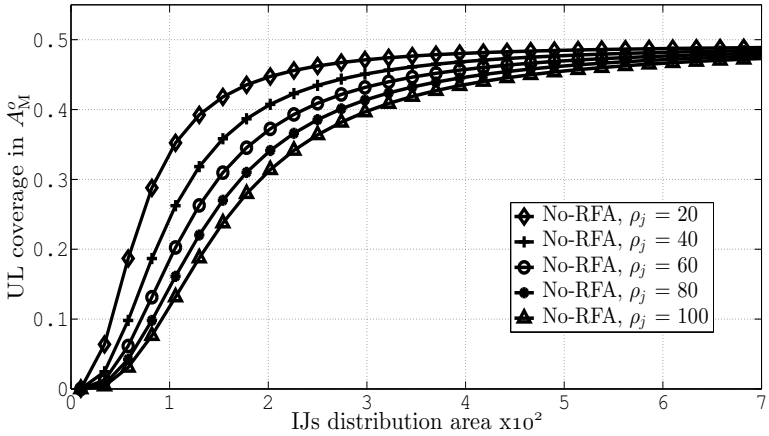

Figure 6. UL coverage against radius for IJs distribution area, without employing RFA.

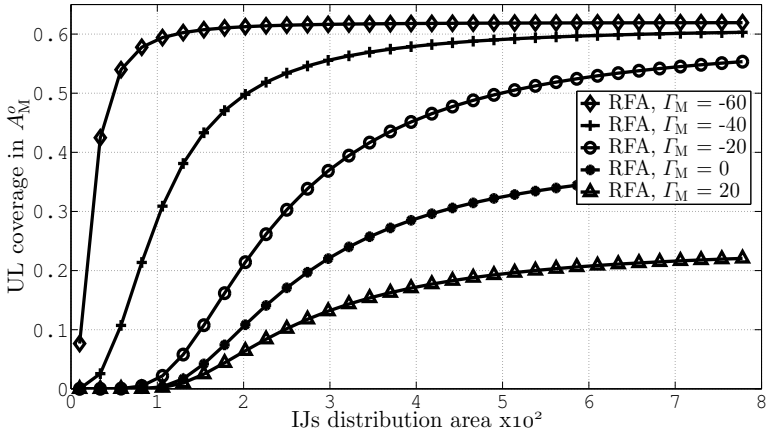

Figure 7. UL coverage against radius for IJs distribution area, with RFA.

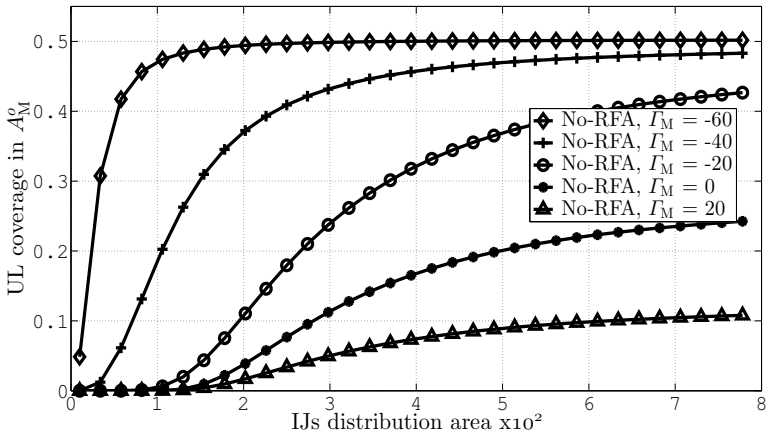

Figure 8. UL coverage against radius for IJs distribution area, without employing RFA.

5. Conclusions

UL coverage of multi-tier HetNets was discussed, in the case of ICI and IJs-I intervention. The paper assumes standardized deployment of MBSs, SBSs, users, and IJs using IHPPPs. The results were created by evaluating various parameters of the network, such as IJs' transmit power, distance, distribution area and SIR threshold with and without RFA jobs. Our findings demonstrate that

UL distribution reduces with the rise in strength and intensity conveyed by IJs. Furthermore, the investigations also indicate a higher SIR level reducing the UL area. In addition, owing to improved ICI and IJs-I reduction, it was found that RFA results in higher UL coverage as compared with the No-RFA case.

Future extensions of this work are listed next

1. UL coverage can be further improved with inclusion of decoupled user associations. It can be used in conjunction with RFA to help in reduction of ICI and IJs-I.
2. In this paper, we have considered jamming to affect the wide band. However, jamming of only certain portion of the band may be investigated as a future work.

Author Contributions: Conceptualization: M.S.H., M.Q. and F.M.; methodology, M.S.H.; software: M.S.H., F.M. and M.Q.; validation: F.M. and M.I.; formal analysis, M.S.H., M.Q. and F.M.; investigation: M.S.H., M.Q., F.M. and M.I.; data curation: M.S.H. and M.Q.; writing—original draft preparation, M.S.H., M.Q., F.M., and M.I.; supervision: F.M., and M.I.; project administration: M.S.H. and M.Q.; funding acquisition: S.K. All authors have read and agreed to the published version of the manuscript.

Funding: Following are results of a study on the "Leaders in INdustry-university Cooperation +" Project, supported by the Ministry of Education and National Research Foundation of Korea.

Conflicts of Interest: The authors declare no conflict of interest.

Appendix A. Proof of the LT of (4)

The LT of interference received from MBS-tier, $\mathcal{L}_{I_{\mathrm{M},A}}(s)$, in A, is obtained as

$$\mathcal{L}_{I_{\mathrm{M},A}}(s) \overset{(a)}{=} \mathrm{E}_{I_{\mathrm{M},A}}\left[\exp\left(-I_{\mathrm{M},A}s\right)\right]\Big|_{s=\frac{r_{\mathrm{M}}^{\beta}\Gamma_{\mathrm{M}}}{P_{t,\nu}^{\mathrm{UL}}}}$$

$$\overset{(b)}{=} \mathrm{E}_{I_{\mathrm{M},A},|h_l|^2}\left[\exp\left(-s\sum_{l\in\phi_{\mathrm{M}}}P_{t,\mathrm{M}}|h_l|^2 r_l^{-\beta}\right)\right]$$

$$\overset{(c)}{=} \mathrm{E}_{I_{\mathrm{M},A},|h_l|^2}\left[\prod_{l\in\phi_{\mathrm{M}}}\exp\left(-|h_l|^2\gamma_{\circ}\Gamma_{\mathrm{M}}r_{\mathrm{M}}^{\beta}r_l^{-\beta}\right)\right]$$

$$\overset{(d)}{=} \mathrm{E}_{I_{\mathrm{M},A}}\left[\prod_{l\in\phi_{\mathrm{M}}}\mathrm{E}_{|h_l|^2}\exp\left(-|h_l|^2\gamma_{\circ}\Gamma_{\mathrm{M}}r_{\mathrm{M}}^{\beta}r_l^{-\beta}\right)\right]$$

$$\overset{(e)}{=} \mathrm{E}_{I_{\mathrm{M},A}}\left[\prod_{l\in\phi_{\mathrm{M}}}\frac{1}{1+\gamma_{\circ}\Gamma_{\mathrm{M}}\left(\frac{r_l}{r_{\mathrm{M}}}\right)^{-\beta}}\right]$$

$$\overset{(f)}{=} \exp\left(-2\pi\rho_{\mathrm{M}}\int_{y}^{d2}\frac{r_l dr_l}{1+\left(\frac{r_l}{\left(\gamma_{\circ}\Gamma_{\mathrm{M}}\right)^{1/\beta}r_{\mathrm{M}}}\right)^{\beta}}\right)$$

$$\overset{(g)}{=} \exp\left(-\pi\rho_{\mathrm{M}}\left(\gamma_{\circ}\Gamma_{\mathrm{M}}\right)^{2/\beta}r_{\mathrm{M}}^{2}\int_{\left(\frac{y}{\left(\gamma_{\circ}\Gamma_{\mathrm{M}}\right)^{1/\beta}r_{\mathrm{M}}}\right)^{2}}^{\left(\frac{d_2}{\gamma_{\circ}\Gamma_{\mathrm{M}}^{1/\beta}r_{\mathrm{M}}}\right)^{2}}\frac{du}{1+(u)^{\beta/2}}\right)$$

Here, Step (a) follows the LT definition [3], Step (b) is obtained by substituting the value of $I_{\mathrm{M},A} = \sum_{l\in\phi_{\mathrm{M}}} P_{t,\mathrm{M}}|h_l|^2 r_l^{-\beta}$, into Step ($a$), Step ($c$) is approached by putting the value of s, Step (e) is approached by calculating LT of Step (d) with respect to h_j, Step (f) is approached by using probability generating functional (PGFL) of IHPPP [33], Step (g) is approached by putting $u = \left(\frac{r_l}{(\gamma_\circ \Gamma_{\mathrm{M}})^{1/\beta} r_{\mathrm{M}}}\right)^2$ in Step (f). Finally, (4) is approached by calculating Gauss-hypergeometric approximation of Step (g).

Appendix B. Proof of the LT of (17)

$$\mathcal{L}_{I^{\mathrm{UL}}_{\phi_{\mathrm{M}},A^c_{\mathrm{M}}}}(s) = \mathrm{E}_{I^{\mathrm{UL}}_{\phi_{\mathrm{M}},A^c_{\mathrm{M}}}}\left[\exp\left(-I^{\mathrm{UL}}_{\phi_{\mathrm{M}},A^c_{\mathrm{M}}} s\right)\right]\Big|_{s=\frac{r_{\mathrm{M}}^{\beta}\Gamma_{\mathrm{M}}}{P^{\mathrm{UL}}_{t,\nu}}}$$

$$= \mathrm{E}_{I^{\mathrm{UL}}_{\phi_{\mathrm{M}},A^c_{\mathrm{M}}},|h_l|^2}\left[\exp\left(-s\sum_{l\in\phi_{\mathrm{M}}} P^{\mathrm{UL}}_{t,\nu}|h_l|^2 r_l^{-\beta}\right)\right]$$

$$= \mathrm{E}_{I^{\mathrm{UL}}_{\phi_{\mathrm{M}},A^c_{\mathrm{M}}},|h_l|^2}\left[\prod_{l\in\phi_{\mathrm{M}}} \exp\left(-|h_l|^2\Gamma_{\mathrm{M}} r_{\mathrm{M}}^{\beta} r_l^{-\beta}\right)\right]$$

$$= \mathrm{E}_{I^{\mathrm{UL}}_{\phi_{\mathrm{M}},A^c_{\mathrm{M}}}}\left[\prod_{l\in\phi_{\mathrm{M}}} \mathrm{E}_{|h_l|^2}\exp\left(-|h_l|^2\Gamma_{\mathrm{M}} r_{\mathrm{M}}^{\beta} r_l^{-\beta}\right)\right]$$

$$= \mathrm{E}_{I^{\mathrm{UL}}_{\phi_{\mathrm{M}},A^c_{\mathrm{M}}}}\left[\prod_{l\in\phi_{\mathrm{M}}} \frac{1}{1+\Gamma_{\mathrm{M}}\left(\frac{r_l}{r_{\mathrm{M}}}\right)^{-\beta}}\right]$$

$$= \exp\left(-2\pi\rho_{\mathrm{M}}\int_y^{d_1} \frac{r_l dr_l}{1+\left(\frac{r_l}{\Gamma_{\mathrm{M}}^{1/\beta} r_{\mathrm{M}}}\right)^{\beta}}\right)$$

$$= \exp\left(-\pi\rho_{\mathrm{M}}\Gamma_{\mathrm{M}}^{2/\beta} r_{\mathrm{M}}^2 \int_{\left(\frac{y}{\Gamma_{\mathrm{M}}^{1/\beta} r_{\mathrm{M}}}\right)^2}^{\left(\frac{d_1}{\Gamma_{\mathrm{M}}^{1/\beta} r_{\mathrm{M}}}\right)^2} \frac{du}{1+(u)^{\beta/2}}\right)$$

Finally, we obtain (17) by calculating Gauss-hypergeometric approximation of Step (f).

References

1. Da Costa, D.B.; Duong, T.Q.; Imran, M.A.; Ngo, H.Q.; Yang, N.; Dobre, O.A. Modeling, analysis, and design of 5G ultra-dense networks. *IEEE Access* **2019**, *7*, 18894–18898. [CrossRef]
2. Andrews, J.G.; Buzzi, S.; Choi, W.; Hanly, S.V.; Lozano, A.; Soong, A.C.; Zhang, J.C. What will 5G be? *IEEE J. Sel. Areas Commun.* **2014**, *32*, 1065–1082. [CrossRef]
3. Błaszczyszyn, B.; Haenggi, M.; Keeler, P.; Mukherjee, S. *Stochastic Geometry Analysis of Cellular Networks*; Cambridge University Press: Cambridge, UK, 2018.

4. Abbas, Z.H.; Abbas, G.; Haroon, M.S.; Muhammad, F.; Kim, S. Proactive uplink interference mitigation in HetNets stressed by uniformly distributed wideband jammers. *Electronics* **2019**, *8*, 1496. [CrossRef]
5. Mirkovic, J.; Reiher, P. A taxonomy of DDoS attack and DDoS defense mechanisms. *ACM SIGCOMM Comput. Commun. Rev.* **2004**, *34*, 39–53. [CrossRef]
6. Jover, R.P. Security attacks against the availability of LTE mobility networks: Overview and research directions. In Proceedings of the International Symposium on Wireless Personal Multimedia Communication (WPMC), Atlantic City, NJ, USA, 24–27 June 2013; pp. 1–9.
7. Huo, Y.; Fan, X.; Ma, L.; Cheng, X.; Tian, Z.; Chen, D. Secure communications in tiered 5G wireless networks with cooperative jamming. *IEEE Trans. Wirel. Commun.* **2019**, *18*. [CrossRef]
8. Jundong, W. Complex environment noise barrage jamming effects on airborne warning radar. *Am. J. Remote Sens.* **2018**, *6*, 59–63. [CrossRef]
9. Viterbi, A. A robust ratio-threshold technique to mitigate tone and partial band jamming in coded MFSK systems. In Proceedings of the MILCOM 1982-IEEE Military Communications Conference-Progress in Spread Spectrum Communications, Boston, MA, USA, 17–20 October 1982; Volume 1, pp. 22–24.
10. Haroon, M.S.; Ahmad, S.; Khan, J.A. LLR-based erasure decoding of SFH-MFSK in the presence of tone jamming. In Proceedings of the 11th International Bhurban Conference on Applied Sciences & Technology (IBCAST), Islamabad, Pakistan, 14–18 January 2014; pp. 453–457.
11. Girke, F.; Kurtz, F.; Dorsch, N.; Wietfeld, C. Towards resilient 5G: Lessons learned from experimental evaluations of LTE uplink jamming. In Proceedings of the 2019 IEEE International Conference on Communications Workshops (ICC Workshops), Shanghai, China, 20–24 May 2019; pp. 1–6.
12. Ham, C.V.; Scoughton, T.E. Radio Frequency Jammer. U.S. Patent 7,318,368, 15 January 2008.
13. Wang, S.; Gao, Y.; Sha, N.; Zhang, G.; Zang, G. Physical layer security in *K*-tier heterogeneous cellular networks over nakagami-*m* channel during uplink and downlink phases. *IEEE Access* **2019**, *7*, 14581–14592. [CrossRef]
14. Muhammad, F.; Haroon, M.S.; Abbas, Z.H.; Abbas, G.; Kim, S. Uplink interference management for HetNets stressed by clustered wide-band jammers. *IEEE Access* **2019**, *7*, 182679–182690. [CrossRef]
15. Soret, B.; De Domenico, A.; Bazzi, S.; Mahmood, N.H.; Pedersen, K.I. Interference coordination for 5G new radio. *IEEE Wirel. Commun.* **2017**, *25*, 131–137. [CrossRef]
16. Zou, S.; Liu, N.; Pan, Z.; You, X. Joint power and resource allocation for non-uniform topologies in heterogeneous networks. In Proceedings of the 83rd Vehicular Technology Conference (VTC Spring), Nanjing, China, 15–18 May 2016; pp. 1–5.
17. Han, T.; Gong, J.; Liu, X.; Islam, S.R.; Li, Q.; Bai, Z.; Kwak, K.S. On downlink NOMA in heterogeneous networks with non-uniform small cell deployment. *IEEE Access* **2018**, *6*, 31099–31109. [CrossRef]
18. Haroon, M.S.; Abbas, Z.H.; Abbas, G.; Muhammad, F. Analysis of interference mitigation in heterogeneous cellular networks using soft frequency reuse and load balancing. In Proceedings of the 28th International Telecommunication Networks and Applications Conference (ITNAC), Sydney, NSW, Australia, 21–23 November 2018; pp. 1–6.
19. Haroon, M.S.; Abbas, Z.H.; Abbas, G.; Muhammad, F. Coverage analysis of ultra-dense heterogeneous cellular networks with interference management. *Wirel. Netw.* **2019**, *26*, 2013–2025. [CrossRef]
20. Hashima, S.; Muta, O.; Alghonimey, M.; Shalaby, H.; Frukawa, H.; Elnoubi, S.; Mahmoud, I. Area spectral efficiency performance comparison of downlink fractional frequency reuse schemes for MIMO heterogeneous networks. In Proceedings of the International Conference on Information Science, Electronics and Electrical Engineering, Hokkaido, Japan, 26–28 April 2014; Volume 2, pp. 1005–1010.
21. Lichtman, M.; Poston, J.D.; Amuru, S.; Shahriar, C.; Clancy, T.C.; Buehrer, R.M.; Reed, J.H. A communications jamming taxonomy. *IEEE Secur. Privacy* **2016**, *14*, 47–54. [CrossRef]
22. Gecgel, S.; Goztepe, C.; Kurt, G.K. Jammer detection based on artificial neural networks: A measurement study. In Proceedings of the ACM Workshop on Wireless Security and Machine Learning, Miami, FL, USA, 15–17 May 2019; pp. 43–48.
23. Zhang, L.; Restuccia, F.; Melodia, T.; Pudlewski, S.M. Jam sessions: Analysis and experimental evaluation of advanced jamming attacks in MIMO networks. In Proceedings of the Twentieth ACM International Symposium on Mobile Ad Hoc Networking and Computing, Catania, Italy, 2–5 July 2019; pp. 61–70.
24. Ciuonzo, D.; Aubry, A.; Carotenuto, V. Rician MIMO channel-and jamming-aware decision fusion. *IEEE Trans. Signal Process.* **2017**, *65*, 3866–3880. [CrossRef]

25. Haroon, M.S.; Muhammad, F.; Abbas, G.; Abbas, Z.H.; Hassan, A.K.; Waqas, M.; Kim, S. Interference management in ultra-dense 5G networks with excessive drone usage. *IEEE Access* **2020**, *8*, 102155–102164. [CrossRef]
26. Liu, K.H.; Yu, T.Y. Performance of off-grid small cells with non-uniform deployment in two-tier HetNet. *IEEE Trans. Wirel. Commun.* **2018**, *17*, 6135–6148. [CrossRef]
27. Muhammad, F.; Abbas, Z.H.; Li, F.Y. Cell association with load balancing in nonuniform heterogeneous cellular networks: Coverage probability and rate analysis. *IEEE Trans. Veh. Technol.* **2016**, *66*, 5241–5255. [CrossRef]
28. Ijaz, A.; Hassan, S.A.; Zaidi, S.A.R.; Jayakody, D.N.K.; Zaidi, S.M.H. Coverage and rate analysis for downlink HetNets using modified reverse frequency allocation scheme. *IEEE Access* **2017**, *5*, 2489–2502. [CrossRef]
29. Ejaz, W.; Anpalagan, A.; Imran, M.A.; Jo, M.; Naeem, M.; Qaisar, S.B.; Wang, W. Internet of Things (IoT) in 5G wireless communications. *IEEE Access* **2016**, *4*, 10310–10314. [CrossRef]
30. Li, S.; Da Xu, L.; Zhao, S. 5G Internet of Things: A survey. *J. Ind. Inf. Integr.* **2018**, *10*, 1–9. [CrossRef]
31. Farahani, B.; Firouzi, F.; Chang, V.; Badaroglu, M.; Constant, N.; Mankodiya, K. Towards fog-driven IoT eHealth: Promises and challenges of IoT in medicine and healthcare. *Future Gen. Comput. Syst.* **2018**, *78*, 659–676. [CrossRef]
32. Bovenzi, G.; Ciuonzo, D.; Persico, V.; Pescapè, A.; Rossi, P.S. IoT-enabled distributed detection of a nuclear radioactive source via generalized score tests. In *International Symposium on Signal Processing and Intelligent Recognition Systems*; Springer: Berlin, Germany, 2018; pp. 77–91.
33. Jiang, X.; Zheng, B.; Zhu, W.P.; Wang, L.; Zou, Y. Large system analysis of heterogeneous cellular networks with interference alignment. *IEEE Access* **2018**, *6*, 8148–8160. [CrossRef]
34. Haroon, M.S.; Abbas, Z.H.; Muhammad, F.; Abbas, G. Analysis of coverage-oriented small base station deployment in heterogeneous cellular networks. *Phys. Commun.* **2020**, *38*, 100908. [CrossRef]
35. Haroon, M.S.; Abbas, Z.H.; Muhammad, F.; Abbas, G. Coverage analysis of cell-edge users in heterogeneous wireless networks using Stienen's model and RFA scheme. *Int. J. Commun. Syst.* **2020**, *33*, e4147. [CrossRef]
36. Jacob, P.; James, A.; Madhukumar, A.S. Downlink capacity improvement and interference reduction through reverse frequency allocation. In Proceedings of the 2012 IEEE International Conference on Communication Systems (ICCS), Singapore, 21–23 November 2012; pp. 329–333.
37. Arif, M.; Wyne, S.; Navaie, K.; Haroon, M.S.; Qureshi, S. Clustered jamming in aerial HetNets with decoupled access. *IEEE Access* **2020**, *8*, 142218–142228. [CrossRef]
38. Haenggi, M. *Stochastic Geometry for Wireless Networks*; Cambridge University Press: Cambridge, UK, 2012.